

AD-A245 902



2

A PHYSICALLY BASED FRACTIONAL CLOUDINESS PARAMETERIZATION

David A. Randall and Qingqiu Shao¹

and

Chin-Hoh Moeng²

DTIC
ELECTE
FEB 10 1992
D D

¹Department of Atmospheric Science
Colorado State University
Fort Collins, Colorado 80523

²National Center for Atmospheric Research
Boulder, Colorado 80307

N00014-89-J-1364

1. Introduction

We have developed a bulk PBL model with a simple internal vertical structure and a simple second-order closure, designed for use as a PBL parameterization in a large-scale model. The turbulent fluxes in the interior of the PBL are parameterized using the "convective mass flux" concept introduced by Arakawa (1969) and adopted in many subsequent studies. Fig. 1 summarizes the conceptual pedigree of this "second-order bulk model" (S.O.B.), relative to earlier models used in boundary-layer and cumulus parameterizations. A sketch of the model's formulation is as follows:

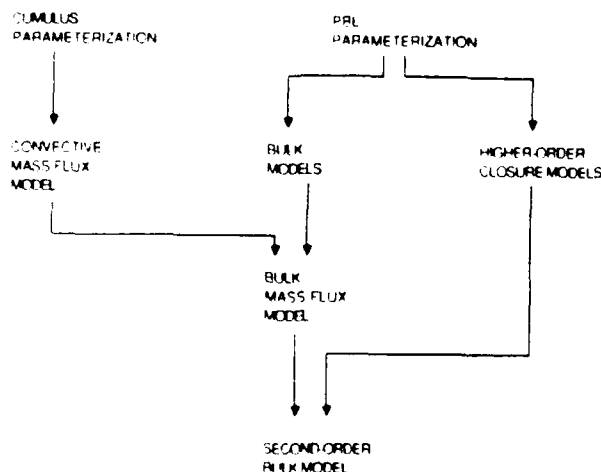


Figure 1: Diagram summarizing the relationship of the present model to earlier models used in boundary-layer and cumulus parameterizations.

The basic framework of the model is shown in Fig. 2. The level just above the PBL top is denoted by subscript B+, while the Earth's surface is denoted by S-. We define an infinitesimal "entrainment layer" just below the PBL top, and an infinitesimal "ventilation layer" just above the Earth's surface. The concept of an entrainment layer is motivated by the observations of Caughey *et al.* (1982) and Nicholls and Turton (1986), who described it as a thin region of weak organized vertical motions and vigorous small-scale mixing. The ventilation layer is more conventionally known as the surface layer.

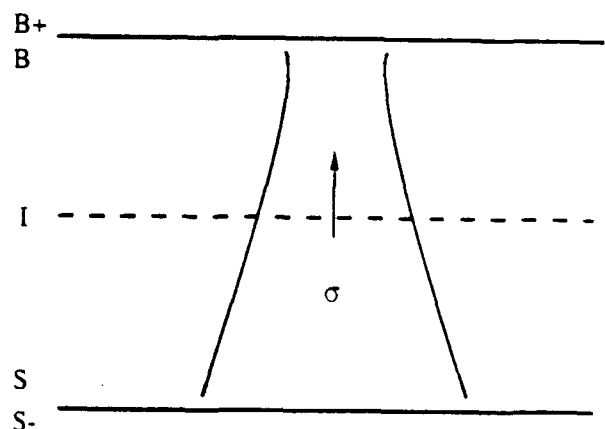


Figure 2: Diagram illustrating the assumed structure of the PBL. The interior, which is represented by two layers, is bounded above by a thin entrainment layer and below by a thin ventilation layer. Convective circulations occur, with rising branches occupying fractional area σ . The ascending and descending branches have different thermodynamic soundings and, therefore, different cloud base levels.

92-02400

The depth of the PBL (in terms of pressure) is prognostically determined, and is denoted by δp_w . The generic variable ψ represents a prognostic intensive scalar such as the dry static energy, the mixing ratio of water, or a component of the horizontal wind. Area-averaged values of ψ are denoted by $\bar{\psi}$. The turbulent flux of ψ , denoted by F_ψ , is defined at the top of the surface layer, and at a level just below the PBL top. These levels are denoted by subscripts S, and B, respectively. The turbulent momentum flux is also defined levels S and B.

An entrainment mass flux, E , carries mass across the PBL top, and is closely related to the turbulent fluxes near the PBL top. Correspondingly, a ventilation mass flux, V , is associated with the surface fluxes; in conventional parlance, V is the product of the surface air density, the surface wind speed, and a transfer coefficient. For both the entrainment and ventilation layers, the model incorporates *diagnostic balances*

for mass, $\bar{\psi}$, and $\bar{\psi}'^2$. The entrainment and ventilation layers are assumed to be thin enough so that such balance conditions are appropriate. Within the ventilation layer, the turbulent fluxes have to be carried by small eddies, since the organized vertical motions associated with the convective circulations must vanish there. The ventilation layer is assumed to be thin, in the sense that the turbulent fluxes at its top are approximately equal to those at the surface. Similarly, within the entrainment layer the organized vertical motions associated with the convective circulations become negligible, so that smaller eddies must again carry the turbulent fluxes. The entrainment layer is assumed to be thin in the sense that the turbulent fluxes at its base are approximately equal to those at the PBL top.

The vertically integrated TKE of the PBL is prognostically determined, and is denoted by e_M . In addition,

the vertically integrated scalar variances, $(\psi')^2_M$, are diagnostically determined. Because the model makes use of these second-order turbulence variables, it can be viewed as a highly simplified second-order closure model with very coarse vertical resolution. The coarse vertical resolution is made palatable (and feasible) by the use of an explicit, prognostic PBL depth. The fine vertical structures that typically occur near the PBL top and the Earth's surface are parametrically included in the model, by methods similar to those used in mixed-layer models. This parametric representation of the vertical structures of the entrainment and ventilation layers is an alternative to explicitly resolving these thin layers; the latter approach is followed in conventional higher-order closure models and is the primary reason that such models require high vertical resolution.

By assuming that the ventilation and entrainment layers at the lower and upper edges of the PBL are dominated by small-scale turbulence in quasiequilibrium, boundary conditions are developed for the rising and sinking branches of the convective circulations, and also for the scalar variances associated with the convective circulations. The convective mass flux and the fractional area covered by updrafts are diagnosed by the model. Fractional cloudiness occurs when the ascending branches are saturated and the descending branches are not.

The convective mass flux is determined using the predicted TKE. In this same spirit, we determine the surface fluxes using a modified bulk formula in which the square root of the TKE takes the place of the wind speed. This allows a natural representation of free convection, and also minimizes the stability dependence of the effective transfer coefficient. Finally, following Siems *et al.* (1990), the entrainment rate is also assumed to be proportional to the square root of the TKE; the proportionality factor depends on the inversion Richardson

number, and also on an additional parameter that represents the effects of evaporative cooling when clouds are present.

A detailed description of the model's formulation is given by Randall and Shao (1990). Here we describe only the method used to determine the fractional area covered by rising motion.

2. A method to determine σ

A key to determining the fractional cloudiness is finding the value of σ , the fractional area covered by rising motion. Previous applications of the mass flux model to boundary layer clouds have not included a method to determine σ . A brief summary of our approach to this problem is as follows:

We assume that, in the interior of the PBL, the turbulent fluxes are entirely due to the convective circulations, with rising branches covering fractional area σ , and sinking branches covering fractional area $1 - \sigma$. Observations based on conditional sampling methods suggest that σ is typically less than 1/2 for the clear convective PBL (e.g., Lenschow and Stephens, 1980), and greater than 1/2 for the cloud-topped PBL (e.g., Nicholls, 1989). Area averages satisfy

$$\overline{(\quad)} = (\quad)_u \sigma + (\quad)_d (1 - \sigma), \quad (1)$$

where an overbar denotes an area average. Subscripts u and d denote upward and downward moving parcels, respectively.

Consider an arbitrary scalar ψ . The turbulent flux of ψ associated with the convective circulations is given by

$$\begin{aligned} F_\psi &= \rho \overline{w'\psi'} = \rho [(w_u - \bar{w})(\psi_u - \bar{\psi})\sigma + (w_d - \bar{w})(\psi_d - \bar{\psi})(1 - \sigma)] \\ &= M_c(\psi_u - \psi_d), \end{aligned} \quad (2)$$

where

$$M_c \equiv \rho \sigma (1 - \sigma) (w_u - w_d) \quad (3)$$

is the convective mass flux.

We enforce consistency between the "mass flux" representation of the fluxes and the boundary conditions on the fluxes at the surface and the PBL top. For brevity, we consider here only the PBL top. The assumption that the entrainment layer is thin yields the familiar "jump" relation between $(F_\psi)_B$ and the entrainment rate:

$$(F_\psi)_B = -E(\bar{\psi}_B - \bar{\psi}_S) - \int_S^B \bar{S}_\psi dz. \quad (4)$$

Here we follow Lilly (1968) by keeping the S_ψ term, which represents a possible concentrated entrainment-layer source of ψ , (e.g., due to radiation). Consistency implies that

$$M_c(\psi_u - \bar{\psi})_B = E\sigma_B(\bar{\psi}_B - \bar{\psi}_S) + \sigma_B \int_S^B \bar{S}_\psi dz \quad (5)$$

At this point, we introduce a mixing parameter χ_E , that relates the properties of the descending air at level B to those of the free atmosphere and the mean state at level B. We include a term that represents the effects of the concentrated source:

$$(\psi_A - \bar{\psi})_B = \chi_E (\bar{\psi}_{B*} - \bar{\psi}_B) + \lambda \int_{z_B}^{z_A} \bar{S}_w dz. \quad (6)$$

Here λ is a coefficient that will be determined later.

The mixing parameter χ_E is closely related to the parameter χ discussed by Siems *et al.* [1989; see also Albrecht *et al.* (1985) and Nicholls and Turton (1986)]. We can interpret χ_E as the value of χ associated with the downdraft air at level B. Since there is a sharp gradient of ψ across the entrainment layer, we expect $0 < \chi_E < 1$.

Comparing (3.6) with (3.7), we find that

$$(-M_{zB} \chi_E + E \sigma_B) (\bar{\psi}_{B*} - \bar{\psi}_B) + (-M_{zB} \lambda + \sigma_B) \int_{z_B}^{z_A} \bar{S}_w dz = 0. \quad (7)$$

In case the source term of (3.8) vanishes, we obtain

$$\chi_E M_{zB} = E \sigma_B. \quad (8)$$

This relationship does not involve ψ ; it must, therefore, apply for *all* ψ . To ensure that (3.9) will be satisfied even when the source term of (3.8) is not zero, we must choose

$$\lambda = \sigma_B / M_{zB}. \quad (9)$$

We can interpret (8) as a "continuity equation" for the eddies. We can use (9) to eliminate λ in (7); the result is:

$$\psi_{AB} = \chi_E \bar{\psi}_{B*} + (1 - \chi_E) \bar{\psi}_B + \frac{\chi_E}{E} \int_{z_B}^{z_A} \bar{S}_w dz. \quad (10)$$

According to (10), the descending air at level B has the properties of the free atmosphere, except as modified by mixing (when $\chi_E < 1$) and by the concentrated source. Caughey *et al.* (1982) and Nicholls (1989) have reported observations of cool downdrafts in the upper portions of stratocumulus cloud sheets. They concluded that the sinking air had been radiatively cooled near the cloud top. Such effects are represented by the S_w term of (10).

The next step is to introduce a further simple relation between χ and σ . We assume that the descending parcels in the convective circulations at level B are formed from the densest parcels available in the entrainment layer. The various parcels are produced by mixing, in various proportions, air from the interior of the PBL with air that has recently been entrained. For the entrainment layer, define χ without a subscript as follows: for each entrainment-layer parcel, χ is the mixing fraction of the air with free-atmospheric properties. Under dry adiabatic mixing, we have

$$s_v(\chi) = \chi \bar{s}_{v*} + (1 - \chi) \bar{s}_{vB}. \quad (11)$$

In such dry adiabatic cases, the entrainment-layer parcels with the lowest virtual dry static energies are those for which χ is zero. [Cloudy cases with phase changes and radiative cooling are discussed later.]

Let the pdf for χ in the entrainment layer be denoted by $\Pi_E(\chi)$. When (11) is satisfied, the average virtual dry static energy of the sinking air emerging from the entrainment layer is

$$(s_{v,d})_B = \frac{\int s_v(\chi) \Pi_E(\chi) d\chi}{\int \Pi_E(\chi) d\chi} \quad (12)$$

We assume that

$$1 - \sigma_B = \int \Pi_E(\chi) d\chi. \quad (13)$$

Use of (13) in (12) gives

$$(s_{v,d})_B (1 - \sigma_B) = \int s_v(\chi) \Pi_E(\chi) d\chi. \quad (14)$$

Simple algebra leads to

$$E \sigma_B (1 - \sigma_B) = M_{zB} \int \chi \Pi_E(\chi) d\chi. \quad (15)$$

Parcels with properties very close to those of the free atmosphere itself make up only a tiny fraction of all the parcels available in the entrainment layer at any given time, so that

$\Pi_E(\chi)$ is very small for values of χ near one, and increases significantly only as χ decreases to values near zero.

Suppose that $\Pi_E(\chi)$ is zero for $\chi_B \leq \chi \leq 1$, and assumes a constant value $\hat{\Pi}_E$ for $0 \leq \chi \leq \chi_B$. Clearly, we must require that

$$\chi_B \hat{\Pi}_E = 1. \quad (16)$$

The PBL is normally capped by an inversion, so that the densest parcels available are those for which χ is near zero. A straightforward analysis leads to

$$\sigma_B = \frac{1}{2 \hat{\Pi}_E \frac{E}{M_{zB}} + 1}. \quad (17)$$

If the mean virtual dry static energy should happen to decrease upward across the entrainment layer, the densest parcels available will have $\chi \equiv \chi_B$. For such a statically unstable entrainment layer, we find that

$$\sigma_B = \frac{1}{2 \hat{\Pi}_E \frac{E}{M_{zB}} - 1}. \quad (18)$$

A similar analysis can be given for the ventilation layer, allowing for both stable and unstable cases. (Randall and Shao, 1990).

Suppose that M_c and σ are independent of height. By combining our results for the ventilation and entrainment layers, we can derive expressions for both M_c and σ . The forms of the resulting expressions guarantee that $M_c \geq 0$ and $0 \leq \sigma \leq 1$. Plots are given in Fig. 3. In all cases, σ decreases as η increases. This means that *strong entrainment is associated with small σ* . When the ventilation layer is unstable and the entrainment layer is stable, the normalized mass flux decreases as η increases. The reverse is true when the ventilation layer is stable and the entrainment layer is unstable. When both layers are unstable, the normalized mass flux is maximized when $\eta = 1$. When both layers are stable, the normalized mass flux is independent of η .

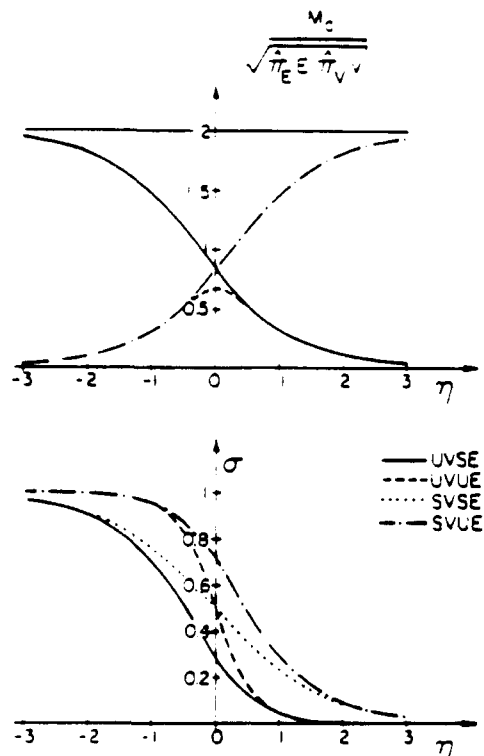


Figure 3: Plots of σ and the normalized mass flux,

$\frac{M_c}{\sqrt{\pi_E E} \sqrt{\pi_V V}}$, as functions of $\eta \equiv \frac{\pi_E E}{\pi_V V}$. "UVSE" denotes unstable ventilation layer with stable entrainment layer; "UVUE" denotes unstable ventilation layer with unstable entrainment layer; "SVSE" denotes stable ventilation layer with stable entrainment layer; and finally "SVUE" denotes stable ventilation layer with unstable entrainment layer.

Phase change processes in clouds can be included in the above analysis without introducing any substantive changes other than minor additional complexity. When radiative cooling occurs in the entrainment layer, (11) must be modified to take into account the radiatively induced moist static energy decrease that each parcel experiences, as a function of χ . We can write

$$h(\chi) = \chi \bar{h}_s + (1 - \chi) \bar{h}_e + \delta h_s(\chi), \quad (19)$$

where h is the moist static energy, and $\delta h_s(\chi)$ represents the effects of radiation on the parcel's moist static energy. We can show that, if $\delta h_s(\chi)$ is independent of χ for the range of χ in question, the following simple relation applies between $\delta h_s(\chi)$ and $\overline{\Delta R}$, the area-averaged radiative flux "jump" across the entrainment layer:

$$\sigma_s \overline{\Delta R} = -M_c \delta h_s. \quad (20)$$

For a given distribution of $\delta h_s(\chi)$, we can work out $\sigma_s(\chi)$. We then identify the densest available parcels, in the usual way.

3. Comparison with large-eddy model results

To validate various aspects of the parameterization, we have used large-eddy simulations produced by Moeng (1984, 1986). We now present some preliminary results of this exercise.

Since drizzle is not included in the large-eddy model, total moisture is a conservative variable. "Passive dye" variables were carried as additional conservative tracers. We have tested our assumptions of conservative mixing in the entrainment layer by using moisture and dye. First we chose model levels to correspond to "B" and "B+". For the cases shown here, the levels used were 40 and 44, respectively. The vertical resolution used was 12.5 m, so these levels corresponded to heights of 500 m and 550 m. By averaging over the domain, we computed mean values for the dye and moisture variables at B and B+. Then, for each individual grid volume found at levels 41 - 43, we computed the two values of χ corresponding to the local mixing ratios of dye and moisture. According to our assumptions, these two values of χ should agree, and of course all values of χ should be between zero and one. Fig. 4 shows that the results are quite satisfactory.

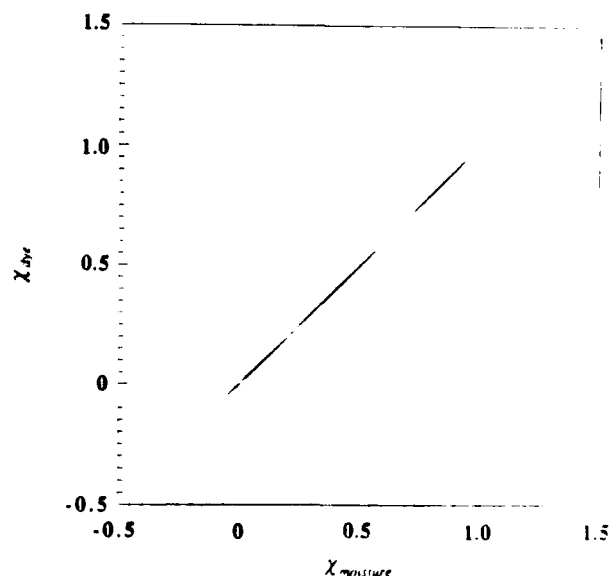


Figure 4: Scatter diagram showing the values of χ obtained from total moisture and dye, respectively, based on the large-eddy simulations of Moeng (1986).

Next, we used the value of χ computed from the moisture field to infer $\delta h_p(\chi)$ from (19). Fig. 5 shows the results, in units of degrees (we have divided by the specific heat at constant pressure). For most values of χ , $\delta h_p(\chi)$ is negative, as we would expect. The values are near -0.1 K. For small values of χ , however, we obtained positive values of $\delta h_p(\chi)$. Further inspection of the model results shows that, although cooling dominates, radiative heating does in fact occur locally at a significant number of grid points near cloud top. The reasons for this are currently being investigated.

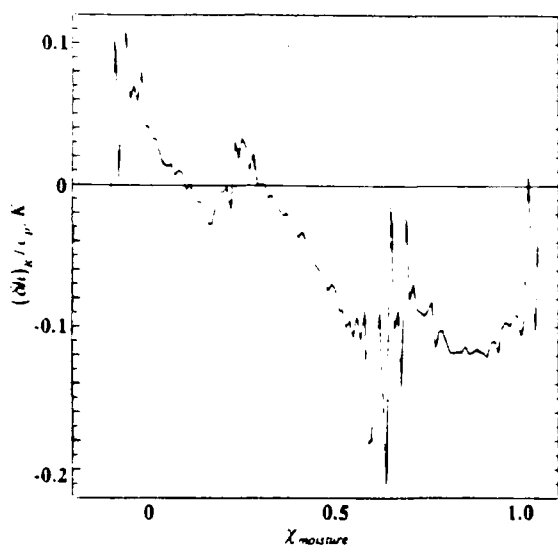


Figure 5: Values of $\delta h_p(\chi)$ plotted as a function of χ , based on the large-eddy simulations of Moeng (1986).

4. Conclusions

We have presented what amounts to very simple second-order-closure model that makes use of an explicit (but highly idealized) description of a turbulent eddy: the "convective circulation." In adopting this approach, we have necessarily abandoned any pretense that the second-order closure is so general that it can apply to any type of turbulent boundary layer. On the other hand, we have benefitted by being able to use mechanistic ideas about the dynamics of individual turbulent elements, which would be difficult or impossible to express in the purely statistical framework of a conventional second-order-closure model.

At present, we are analyzing tethered balloon data collected at San Nicolas Island during FIRE, to determine the applicability of the model to the observations. We are also performing a further analysis of Moeng's large-eddy simulations. Further results will be presented at the Conference.

ACKNOWLEDGEMENTS

Support for this research was provided by NASA's Climate Program under Grant NAG-1-893, and by the Office of Naval Research under Contract N00014-89-J-1364. Computing resources were provided by the Numerical Aerodynamic Simulation Facility at NASA/Ames.

REFERENCES

- Albrecht, B. A., R. S. Penc, and W. H. Schubert, 1985: An observational study of cloud-topped mixed layers. *J. Atmos. Sci.*, **42**, 800-822.
- Arakawa, A., 1969: Parameterization of cumulus convection. *Proc. WMO-IUGG Symp. Numerical Weather Prediction*, Tokyo, 26 November - 4 December, 1968, Japan Meteor. Agency, IV, 8, 1-6.
- Caughey, S. J., B. A. Crease, and W. T. Roach, 1982: A field study of nocturnal stratocumulus: II. Turbulence structure and entrainment. *Quart. J. Roy. Meteor. Soc.*, **108**, 125-144.
- Lenschow, D. H., and P. L. Stephens, 1980: The role of thermals in the convective boundary layer. *Bound. Layer Meteor.*, **19**, 509-532.
- Lilly, D. K., 1968: Models of cloud-topped mixed layers under a strong inversion. *Quart. J. Roy. Meteor. Soc.*, **94**, 292-309.
- Moeng, C.-H., 1984: A large-eddy simulation model for the study of planetary boundary-layer turbulence. *J. Atmos. Sci.*, **41**, 2052-2062.
- Moeng, C.-H., 1986: Large-eddy simulation of a stratus-topped boundary layer. Part I: Structure and budgets. *J. Atmos. Sci.*, **43**, 2886-2900.
- Nicholls, S., and J. D. Turton, 1986: An observational study of the structure of stratiform cloud sheets. Part II. Entrainment. *Quart. J. Roy. Meteor. Soc.*, **112**, 461-480.
- Nicholls, S., 1989: The structure of radiatively driven convection in stratocumulus. *Quart. J. Roy. Meteor. Soc.*, **115**, 487-511.
- Siems, S. T., C. S. Bretherton, M. B. Baker, S. Shv, and R. T. Breidenthal, 1989: Buoyancy reversal and cloudtop entrainment instability. Submitted to *Quart. J. Roy. Meteor. Soc.*

Accession For	
NTS CRASH	J
FILE 128	
Classified by	
J. MICHAEL	
By	
D. MICHAEL	
Approved by	
Test	
A-1	

Statement A per telecon
Dr. Robert Abbey GWR/Code 1122
Arlington, VA 2217-5000
NW 2/7/92